https://doi.org/10.5194/egusphere-2022-949
Preprint. Discussion started: 20 September 2022

Rift thermal inheritance in the SW Alps (France): insights from RSCM thermometry and 1D thermal numerical modelling

Naïm Célini [1,2,3], Frédéric Mouthereau[2], Abdeltif Lahfid[3], Claude Gout[1], Jean-Paul Callot[1]

[1] Université de Pau et des Pays de l'Adour, E2S UPPA, CNRS, TotalEnergies, LFCR, Pau, France.

[2] Géosciences Environnement Toulouse, Université de Toulouse Paul Sabatier, CNRS, IRD, Toulouse, France.

[3] Bureau des Recherches Géologiques et Minières, Orléans, France.

Correspondence to: celini.naim@gmail.com

ABSTRACT

Conceptual models of orogenic accretionary prisms assume the increase in peak temperatures (T_{max}) towards the internal domains as crustal rocks are accreted from the lower to the upper plate. Yet, the recognition of pre-orogenic heating events in mountain belts questions the magnitude of thermal overprint during nappe stacking. Using Raman Spectroscopy on Carbonaceous Material (RSCM) to calculate T_{max}, we have investigated the thermal record of Lower Jurassic to Upper Cretaceous strata exposed along the Digne Nappe, at the front of the SW Alps. Our results highlight two groups of depth-dependent temperatures: (1) a regionally extensive constant T_{max} up to 300-330°C measured in the Jurassic succession and (2) regionally variable lower temperature (<150°C) recorded either in the upper Mesozoic, the nappe stack or the syn-orogenic sequence. Modelling shows that the highest paleotemperatures were achieved during the Early Cretaceous (~130 Ma), during the Valaisan-Vocontian rifting, while the lowermost ones reflect syn-orogenic burial in the Alpine foreland basin. This study provides a striking new example where mid-crustal paleotemperatures measured in lower plate sediments now accreted at the thrust front are inherited. Estimated peak thermal gradient of 80-90°C/km requires crustal thickness of ~15 km during the Early Cretaceous, hence placing new constraints for tectonic reconstruction of rift domains and geophysical interpretation of current crustal thickness in the SW Alps. These results call for the careful interpretation of paleothermal data when they are used to identify past collisional events. Where details of basin evolution are lacking high-temperature record may be misinterpreted as syn-orogenic, which can in turn lead to overestimating both orogenic thickening and horizontal displacement in mountain belts.

INTRODUCTION

https://doi.org/10.5194/egusphere-2022-949
Preprint. Discussion started: 20 September 2022

The identification of collisional events through Earth history lies in our capacity to distinguish in the rock record and crustal structure, the effect of crustal thickening among other tectono-magmatic events unrelated to plate convergence. Conceptual models of orogenic accretionary prisms describe the increase of T_{max} from the external fold-and-thrust belts to the internal high-grade metamorphic domains as a result of tectonic burial heating and thermal advection due to nappe stacking and erosion as crustal rocks are accreted (Barr et al., 1991). Therefore, a potential relevant indicator of collision is the onset of heating related to crustal thickening of previously subducted rocks (e.g. Soret et al., 2021). In contrast, it has been shown that mid-crustal temperatures (i.e. at least 300°C) reconstructed in accreted sedimentary rocks can represent rift-related thermal peaks not overprinted by crustal thickening. This has been substantiated in low-convergence collisional orogens such as the Pyrenees (Clerc and Lagabrielle, 2014; Vacherat et al., 2014; Izquierdo-Llavall et al., 2020; Ducoux et al., 2021) and the Iberian Range (Rat et al., 2019) as well as in higher convergence collisional orogens such as Taiwan (Conand et al., 2020). An improved quantification of pre- versus syn-orogenic thermal evolution in orogenic prisms is thus needed to reduce uncertainties on tectonic reconstructions and recognition of past collisional events.

The Western Alps are an archetypal mountain belt formed by crustal accretion of the European and Adria paleomargins that followed the subduction of the Alpine Tethys (e.g. Handy et al., 2010). T_{max} of about 300°C reported from RSCM data in accreted sediments of the lower plate of the orogen (Europe, Fig. 1) are commonly attributed to syn-convergence thermal overprint in the internal (e.g. Lanari et al., 2012) and the external parts of the belt (Deville and Sassi, 2006; Bellanger et al., 2015). The identification of initial rifted margin architecture in the internal domains of the Alps despite later subduction and crustal thickening (e.g. Beltrando et al., 2014), together with issues related to the magnitude of continental subduction argue for tectonic models of collision accounting for improved resolution of pre-collisional evolution (Pleuger and Podladchikov, 2014; Luisier et al., 2019). Although being difficult to establish in the internal domain because of potential overprinting during subduction and collision, the thermal impact of rifting events is expected to be more clearly separated from other tectonic phases at the thrust front but this has never been properly estimated so far.

Here, we focus on the Digne Nappe, carrying a thick Jurassic syn-rift section at the front of the external SW Alps (Gidon, 1997), which lacks thermal constraints. This study combines 80 new RSCM measurements collected at the front of the Digne Nappe along continuous pre-collisional stratigraphic series in the footwall of the accretionary prism. To resolve the timing of pre-orogenic versus syn-orogenic thermal imprints, a set of

https://doi.org/10.5194/egusphere-2022-949
Preprint. Discussion started: 20 September 2022

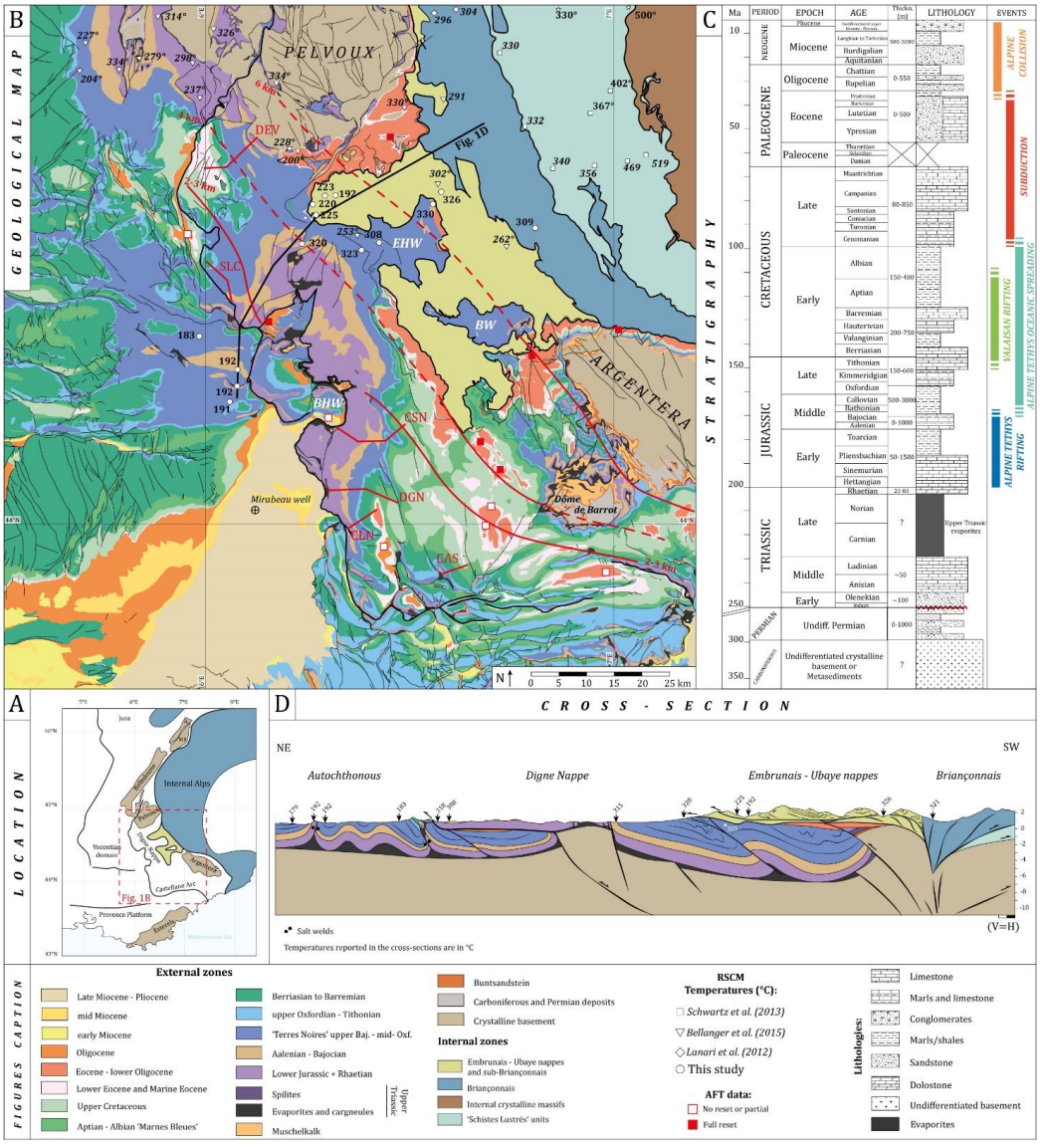

Figure 1: (A) Location of the study area in the regional framework of the Western Alps. (B) Simplified geological map of the SW Alps with the position of the sampled stratigraphic sections and RSCM temperatures from the literature (Lanari et al., 2012; Schwartz et al., 2013), modified from the BRGM geological maps at 1/250000. Red lines are reconstructed isopachs of Cenozoic foreland deposits reconstructed based on published apatite fission-track data (see text for references). BHW=Barles Half Window; BW=Barcelonnette Window and EHW=Embrun Half Window. (C) Simplified synthetic stratigraphic column of the area, modified from Célini et al. (2022). (D) Cross-section through the northern part of the Digne Nappe and the Embrunais-Ubaye nappes containing temperatures from this study. See location in (B).

modelled time-temperature scenarios has been designed. Our results lead to the re-evaluation of the importance of rifting-related, lower plate thermal inheritance, and provide constraints on the palaeogeography and extensional processes in the SW Alps.

https://doi.org/10.5194/egusphere-2022-949
Preprint. Discussion started: 20 September 2022

GEOLOGICAL SETTING

The SW Alps include tectonic units that result from the tectonic inversion of the European margin formed in response of two main extensional phases. The first one, Early Jurassic in age, led to the opening of the Alpine Tethys s.s. (e.g. Manatschal and Müntener, 2009). The second, Late Jurassic – Early Cretaceous in age, appears synchronous with the rifting of the Bay of Biscay and led to opening the Valaisan domain to the NE of the Alpine arc (Beltrando et al., 2012) and renewed extension in the so-called Vocontian Trough of the SW Alps (Graciansky and Lemoine, 1988; Angrand and Mouthereau, 2021). Continental break-up resulted in the formation of the European and Adria passive margins on both sides of the slow-spreading oceanic domain of the Alpine Tethys oriented NE-SW (Lemoine et al., 1986; Graciansky et al., 1989; Mohn et al., 2014; Manatschal et al., 2021). Oceanic spreading lasted until the beginning of the Late Cretaceous as the subduction of the eastern part of the Alpine Tethys started (Coward and Dietrich, 1989; Handy et al., 2010). Convergence in the Western Alps is characterised by two major stages (e.g. Ford et al., 2006). The first one, which occurred before 33.9 Ma corresponds to the displacement of the Alpine accretionary prism to the N-NW (Merle and Brun, 1984; Dumont et al., 2011, 2012). The second one, post 33.9 Ma, corresponds to the onset of collision marked by widespread crustal thickening in the Western Alps. This event is characterised by NW-oriented shortening in the northern Western Alps, while it is directed W- to SW-oriented shortening in the southern Western Alps (Coward and Dietrich, 1989; Fry, 1989; Dumont et al., 2011; Bellahsen et al., 2014).

Currently running between the variscan Pelvoux and Argentera crystalline massifs, the Digne main thrust is oriented NNW-SSE and dies out to the north near the western border of the Pelvoux (Fig. 1). To the east, the hangingwall units of the Digne Nappe are in tectonic contact with the front of the Embrunais-Ubaye (E-U) nappes that are formed by sub-Briançonnais Triassic to upper Eocene sediments overthrusted by upper Cretaceous-Eocene flyschs units (Helminthoid flyschs) emplaced during the Eocene-Oligocene (Kerckhove and Thouvenot, 2010). It turns to an E-W direction in the Castellane Arc to the south (Fig. 1).

The Digne Nappe, forming the SW Alps thrust front, is made of Triassic to Cretaceous series and Eocene-Oligocene foreland remnants transported towards the SW over 20-25 km (Faucher et al., 1988; Gidon, 1997; Lickorish and Ford, 1998). These series belong to the former European passive margin (Baudrimont and Dubois, 1977; Debrand-Passard et al., 1984; Gidon, 1997), highly affected by pre- and syn-orogenic salt tectonics since the Early Jurassic and during its whole history (e.g. Célini et al., 2020, 2021, 2022). As the margin was inverted during the Miocene, Triassic evaporites served as an efficient décollement level for the

https://doi.org/10.5194/egusphere-2022-949
Preprint. Discussion started: 20 September 2022

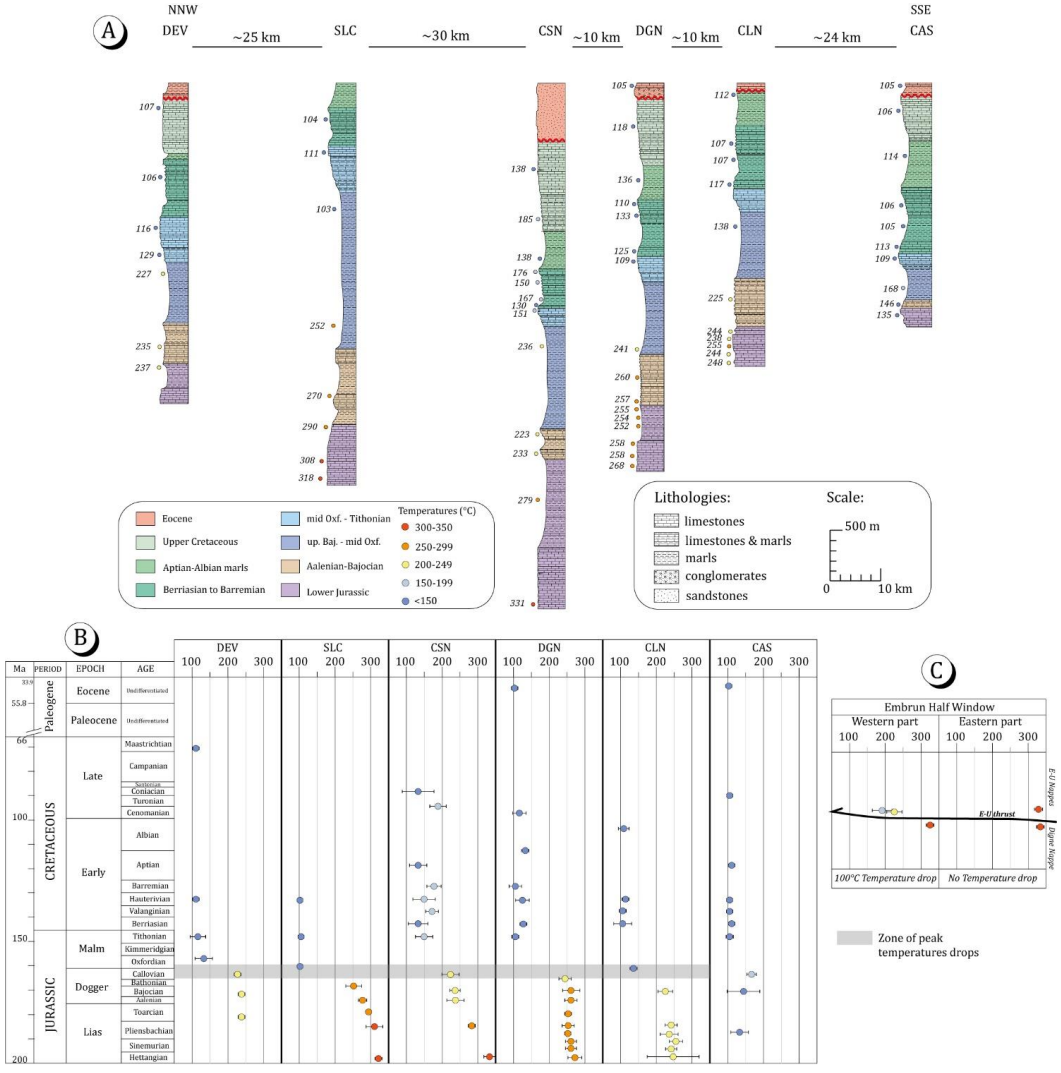

Figure 2: (A) RSCM-derived peak temperatures along the stratigraphic sections at the front of the Digne Nappe. See Data Repository 1 for details about the samples and Fig. 1 for the location of the sections. (B) Evolution of the RSCM temperatures through geological time scale along the sedimentary columns and (C) in two locations of the Embrun Half Window.

Digne Nappe (Gidon and Pairis, 1985; Faucher et al., 1988; Gidon, 1997; Lickorish and Ford, 1998). The latest thick-skinned phase of the Digne Nappe emplacement, forming the SW Alps thrust front, occurred during the Mio-Pliocene since ca. 10 Ma (Ford et al., 2006; Schwartz et al., 2017).

SAMPLES AND METHOD

RSCM thermometry along reconstructed vertical sections

https://doi.org/10.5194/egusphere-2022-949
Preprint. Discussion started: 20 September 2022

We selected six 2.5 to 5 km-thick stratigraphic sections (DEV, SLC, DGN, CSN, CLN, CAS) distributed from NNW to SSE over a distance of 80 km along the Digne thrust front (Fig. 1B). Samples have been retrieved from pre-collisional carbonate deposits of Early Jurassic to Late Cretaceous ages, and in rare occasions in Eocene foreland deposits (CAS and DGN, Fig. 2A). Because the nappe emplacement occurred in the Mio-Pliocene (Schwartz et al., 2017), they are assumed to be representative of original vertical stratigraphic sections prior to thrusting. We applied the RSCM calibration of Lahfid et al. (2010) for temperatures ranging between 200 and 340°C, and added the qualitative analysis of Saspiturry et al. (2020) for lower temperatures between 100 and 180°C. This dataset was complemented by 15 RSCM analyses in the autochthonous units (Fig. 1B) and in the E-U nappes as well as individual spots from the Embrun half window (Fig. 2C). The 80 RSCM-derived T_{max} computed from samples along our sections are assumed to represent either the maximum temperatures acquired during heating related to burial during the passive margin stage coeval to crustal thinning of the European margin, burial by Eocene-to-Miocene foreland sediments or tectonic burial beneath the E-U nappes to the East. To determine the timing of acquisition of our T_{max}, making assumptions of vertical thermal gradients, we took advantage of the existing low-temperature fission-track analyses performed on the Cenozoic sediments (Fig. 1B, Labaume et al., 2008; Jourdan et al., 2013; Schwartz et al., 2017) from which one can estimate the hypothetical maximum thickness of the overburden (depositional or tectonic) at the time of thrusting.

Numerical modelling with basin model

To quantitatively examine which tectonic scenario best reproduces the distinct groups of depth-dependent temperatures across the Digne thrust front, we used 1D numerical modelling TemisFlow® (Doligez et al., 1986) to reconstruct burial histories of decompacted stratigraphic columns and converted them into T_{max} applying different tectonic evolutions. The 3 tested scenarios are (1) burial in the Alpine foreland as the main controlling factor for the T_{max} establishment, (2) rifting during the Early-Middle Jurassic corresponding to crustal thinning from 30 to 8-10 km and lithospheric mantle thinning from 90 to 15 km during the Alpine Tethys rifting event, followed by thermal relaxation and finally burial in the Alpine foreland and (3) two rifting events during the Early-Middle Jurassic (Alpine Tethys rifting) and Late Jurassic-Early Cretaceous (Vocontian-Valaisan rifting) leading to final thicknesses of 8-10 km of crust and 10-15 km of lithospheric mantle also followed by thermal relaxation and burial in the Alpine foreland during the Cenozoic. In the Barles Half Window (Fig. 1B), partially reset AFT ages documented in Miocene marine molasses reveal maximum burial depths of

https://doi.org/10.5194/egusphere-2022-949
Preprint. Discussion started: 20 September 2022

3-4 km (Schwartz et al., 2017), an estimate that includes the thickness of the overlying nappe. Further to the SW, beneath the Digne Nappe, the thickness of the Mio-Pliocene series is constrained by the Mirabeau well to 2 km (Fig. 1, see Graham et al., 2012). We infer that it is 3 km at the Digne thrust front (Fig. 1B). We included the 3 km of eroded Cenozoic sediments to reconstruct the thickness of Cretaceous strata that are now missing in DEV, SLC, CSN and CLN sections.

In the first model, no extensional event is introduced and the sedimentary columns record burial beneath a maximum of 3 km of syn-orogenic deposits, which are partially or completely eroded at present-day. In the second model, the sedimentary columns suffered heating during the Early to Middle Jurassic extensional event (201-169 Ma) as a result of burial and upward advection of the asthenosphere. After this thinning event, the lithosphere cools by thermal relaxation, i.e. the lithosphere-asthenosphere boundary (LAB) deepens. The third model is intended to reproduce two thinning events during the Early-Middle Jurassic (201-169 Ma) and the Late Jurassic-Early Cretaceous (150-129 Ma). After 125 Ma, the lithosphere records thermal relaxation and later, from the Paleogene onwards, flexure and burial in the Alpine foreland basin. As the margin is inverted during the Cenozoic, crustal and mantle thickness are designed to progressively increase to reach initial values, thus mimicking lithosphere thickening during collision.

The temperature at the base of the lithosphere is fixed at 1333°C and we consider a continental crust made with different lithologies in the sedimentary cover (sandstone, limestone, marls, etc.) overlying a crustal basement with homogeneous properties. The rocks physical and thermal properties used in the software TemisFlow® are presented in Table 1. All the sections are detached in the Upper Triassic evaporites, it is thus difficult to estimate the original thickness of these evaporites, especially since they are also involved in salt tectonics since the Early Jurassic (e.g. Célini et al., 2020). We thus assume for every section a reasonable initial thickness of 100 m for the Upper Triassic evaporites. Regarding the Lower and Middle Triassic sandstones and

Lithology	Density ($kg.m^{-3}$)	Thermal conductivity ($W.m^{-1}.°C^{-1}$)	Heat capacity ($J.kg^{-1}.°C^{-1}$)	Radiogenic production ($W.m^{-3}$)
Sandstone	2670	4,6	740	9,5E-07
Limestone	2710	3,57	795	6,2E-07
Marls/limestone alternation	2690	2,76	805	9,6E-07
Marls	2680	2,76	815	1,3E-06
Conglomerate	2350	3,27	812	1,6E-06
Salt	2160	6,1	865	1,0E-08
Crust	2650	3	1150	2,0E-06
Lithospheric mantle	3350	3,3	1200	None

Table 1: Rock properties adopted for modelling with TemisFlow®.

https://doi.org/10.5194/egusphere-2022-949
Preprint. Discussion started: 20 September 2022

limestones, we considered the thickness exposed in a few location of the SW Alps (e.g. Haccard et al., 1989), that is 50 m of Lower Triassic sandstones and 50 m of Middle Triassic limestones.

RESULTS

RSCM Temperatures

RSCM temperatures obtained along the six sections are presented in Fig. 2A and in details in the Suppl. File 1. We systematically observe two temperature trends separated by an abrupt shift of 50 to 100°C (Peak temperature drop in Fig. 2B). The deeper domain, characterised by relatively higher T_{max} ranging between 200 and 340°C, in the Lower Jurassic and Middle Jurassic deposits at reconstructed burial depths between 2 and 4 km, except for the CAS section (Fig. 2A). In contrast, in the Upper Jurassic and Cretaceous post-rift strata as well as in the syn-orogenic deposits, T_{max} are below 150°C. It is worth noting that the 100°C T_{max} drops in section DEV occurs over a few tens of meters, corresponding to a sharp transition in the Middle to Upper Jurassic interval (Fig. 2A). Along the southern CAS section, located in the Castellane Arc, the T_{max} do not exceed 170°C at the base of the section. Temperatures from Middle Jurassic series located farther to the east in the Embrun half window range between 300 and 330°C (Fig. 1). Samples in the Jurassic and Eocene from the E-U nappes, tectonically above the Digne Nappe, in contrast yield notably lower T_{max} between 190 and 225°C (Fig. 2C).

Evidence for rift-related thermal event recorded at the Digne frontal thrust

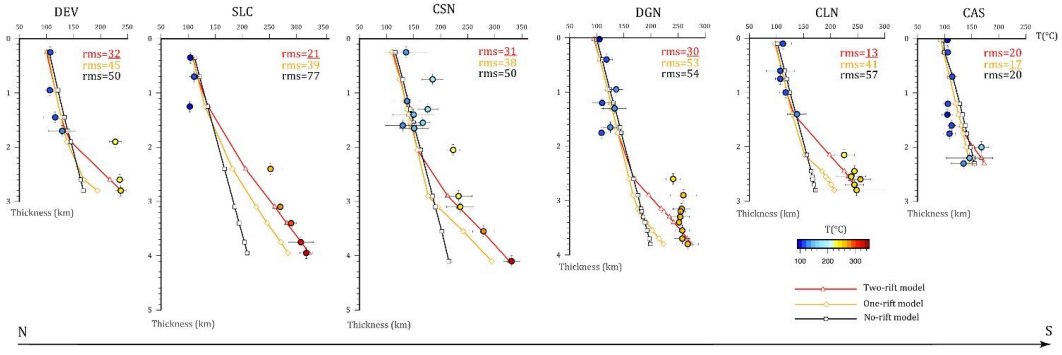

Figure 3: Comparison between observed RSCM temperatures (colour-coded circles) and temperatures computed based on tested tectonic models (Two-rifts, One-rift and No-rift) represented by color-coded lines and symbols. RMS are the root mean square data misfit error calculated for each model. Reconstructed temperature-depth slopes correspond to thermal gradients: 30°C/km (upsection) and 80-90°C/km(downsection). RSCM data are best reproduced for the Two-rifts model and if peak temperatures are achieved during the Early Cretaceous.

https://doi.org/10.5194/egusphere-2022-949
Preprint. Discussion started: 20 September 2022

The T_{max} measured in the uppermost parts of the sections fit with apatite fission-track (AFT) ages from the (para-)autochtonous Eocene strata (CAS, DGN) revealing partially reset ages and therefore indicating temperatures below 120°C. Assuming a post-extension thermal gradient of 30°C/km, T_{max} of 100-150°C found in the upper parts of the sections are likely to reflect burial in the Alpine foreland. However, a similar burial with the same geothermal gradient fails to explain the high T_{max} up to 300-330°C found in deeper Early-Middle Jurassic strata (DEV, SLC, CSN, DGN, CLN sections) as they would imply 6-7 km of foreland sediments at the front and the reset of all AFT ages. In addition, the ~100°C gap between the temperatures in the E-U nappes and those in the Digne Nappe beneath (Fig. 2B), suggests that the emplacement of the nappes stack of the Alpine accretionary wedge is not responsible for the high T_{max} observed in the Digne Nappe. Rather, these temperatures likely represent an older and higher-grade thermal event which produced temperatures too high to be reset by the subsequent Alpine burial. A notable exception is the CAS section that appears consistent with the syn-orogenic burial in the Alpine foreland only.

Results of numerical modelling

The comparison between RSCM data and numerical modelling results is presented in Fig. 3. We have extracted from the tested burial histories experiments in TemisFlow® (Fig. 4) the maximum temperature reached at a given stratigraphic level and geothermal gradients reached in the stratigraphic columns (Fig. 5). To quantitatively evaluate the results, we calculated the root mean square (RMS) data misfit error between model and observations (Fig. 3). Note that we show in figures 3 and 4 results from the third model only (two-rifts), which best fit the measured RSCM temperatures. The reader is referred to the supplementary files for other TemisFlow® experiments. In the first model, that assume peak heating during syn-orogenic burial in the foreland, the fit is good for the uppermost samples but the model fails to reproduce the observed T_{max} above 200°C in deeper samples (Fig. 3 & Suppl. File 2). The only exception is the CAS section which is distinctively colder (Fig. 2 & 3). For the second model that incorporates crustal thinning to 8-10 km and shallowing of the LAB from 90 to 15 km during the Early-Middle Jurassic, the fit is noticeably better (Fig. 3) for the deeper samples with higher temperatures (Suppl. File 3). This is caused by the increased of the crustal geothermal gradient to 70 to more than 90°C/km that results from lithosphere thinning (Suppl. File 4). The third model (Fig. 4), which includes the superimposition of two rifting events in a few tens of million years, present a much better fit of the temperatures both for the shallower and deeper samples (Fig. 3). Burial histories show that the deepest

https://doi.org/10.5194/egusphere-2022-949
Preprint. Discussion started: 20 September 2022

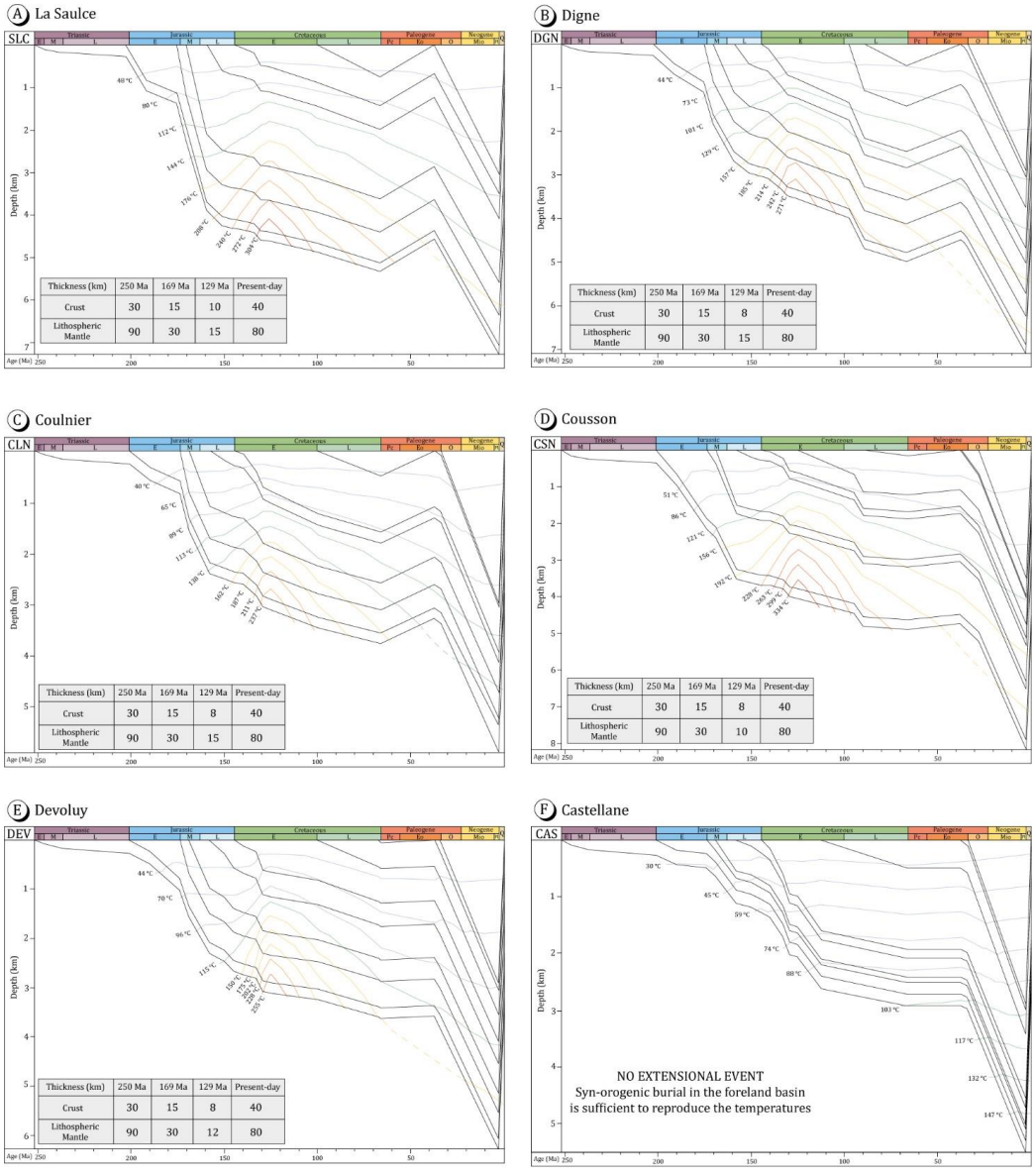

Figure 4: Burial histories from decompacted stratigraphic columns generated with TemisFlow®. Two-Rift hypothesis for A, B, C, D and E and the No-Rift hypothesis for F. See location of each column in Fig. 1 and the detailed stratigraphy of each column in Fig. 2.

sediments record temperature above 230-330°C during the Early Cretaceous (130-110 Ma). Lithosphere thinning reached a climax such that conductive crustal geothermal gradients increased from 50-60°C/km during the Earl-Middle Jurassic to 80-90°C/km during the Early Cretaceous (Fig. 5). The cumulated thermal effect of the Jurassic and Early Cretaceous rifting is required to fit the RSCM data, especially to reproduce the T_{max} beneath 2 km (Fig. 3). The rifting event is followed by thermal relaxation as gradients return to 30°C/km during the Late Cretaceous and burial in the foreland beneath 3 km of Cenozoic deposits. The only exception is the

https://doi.org/10.5194/egusphere-2022-949
Preprint. Discussion started: 20 September 2022

CSN section, which has required 4 km of burial in the foreland to fit the T_{max} of the upper part of the section. This value agrees with another study indicating that Eocene-Oligocene syn-orogenic deposits of the Alpine foreland can have reached around 4 km in that location (Fig. 1B, Labaume et al., 2008). The temperatures of the colder CAS section can be accounted for by any of our scenarios (Fig. 3). However, considering its location in the Castellane Arc (Fig. 1B) characterised by much thinner Jurassic series, it is likely that crustal thinning has remained modest in this area because originally located in the inner domain of the European rifted margin of the Alpine Tethys. We thus favour the scenario without rifting events and with syn-orogenic burial only (Fig. 4F).

The abrupt temperature drop observed along the sections (Fig. 2 and 5) is never well reproduced by the thermal numerical modelling. This can be due to 3D effects, affecting the samples in nature, that can homogenise temperatures or to the presence of evaporites involved in salt tectonics that can largely influence the temperature distribution (e.g. Jensen, 1983; Mello et al., 1995), that are not taken into account in our experiments. This may also be linked to the kinetics of organic matter maturation, not taken into account in our numerical experiments, while the RSCM approach is based on organic matter maturation (e.g. Lahfid et al., 2010).

DISCUSSION

T_{max} explained by decoupled crust-mantle thinning in the SW Alpine foreland

In our preferred scenario, with the best match between numerical experiment and RSCM data, observed T_{max} in the Digne thrust sheet are reached after the initial Jurassic rifting phase, during the second phase of Early Cretaceous rifting, when the overburden is 3-4 km thick and gradients are about 80-90°C/km (Fig. 4). Only a limited combination of crustal thicknesses of 8-10 km and lithospheric mantle thicknesses of 10-15 km (Fig. 4) can reproduce the RSCM data. This scenario implies a significant thinning of the whole lithosphere from 120 to 20 km. This is a result of long-lasting stretching processes that occurred from the Early-Middle Jurassic (201-169 Ma) to the Late Jurassic-Early Cretaceous (150-129 Ma) (Fig. 4). The total crustal stretching (β-factor) is 3-3.75 and reaches 6-9 for the lithospheric mantle. These different values indicate a depth-dependant stretching mechanism. We note that the crustal stretching factor of 3-3.75 fits well crustal thicknesses often observed at the transition between necking and hyper-thinned domains at magma-poor rifted margins (e.g. Tugend et al., 2015). Such observations call for a careful re-examination regarding the initial position of the Digne Nappe in

https://doi.org/10.5194/egusphere-2022-949
Preprint. Discussion started: 20 September 2022

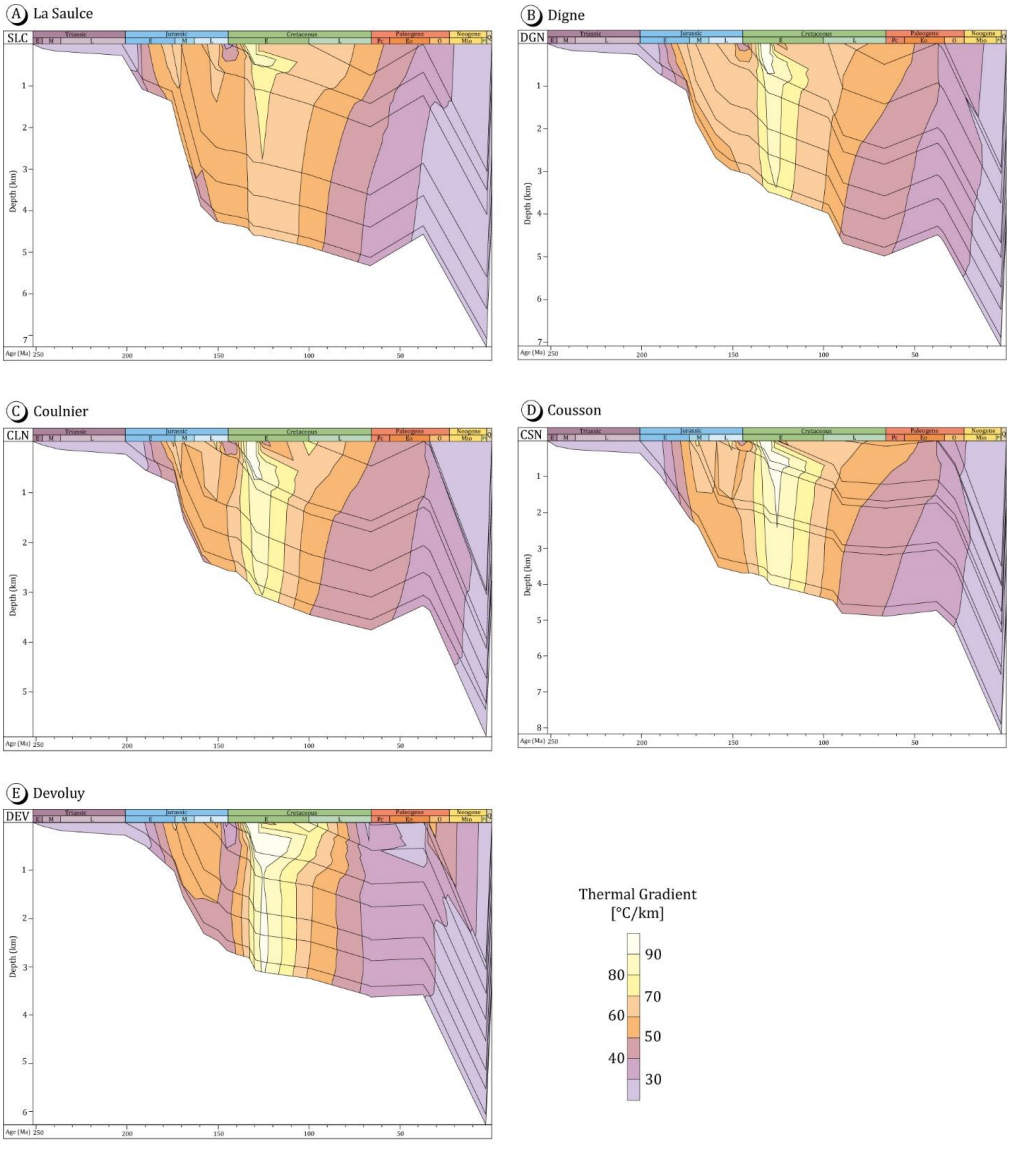

Figure 5: Burial evolution of each sedimentary column and evolution of thermal gradients along the sections. The CAS (Castellane) section is not represented here because the thermal gradient is constantly equal to 30°C/km.

the European rifted margin especially because it was originally located on a very oblique segment (transfer zone) of the margin (Fig. 6).

The high gradients of 80-90 °C/km attained during the peak thermal event (Fig. 5) have been recognized in other inverted rift basins, also Early Cretaceous in age, such as the Pyrenees (e.g. Vacherat et al., 2014) and the Iberian Range (Rat et al., 2019). They have been linked to extreme extension of rifted margins that is expected to be better preserved during collision in the upper plate (e.g. Jourdon et al., 2019; Ternois et al., 2021).

https://doi.org/10.5194/egusphere-2022-949
Preprint. Discussion started: 20 September 2022

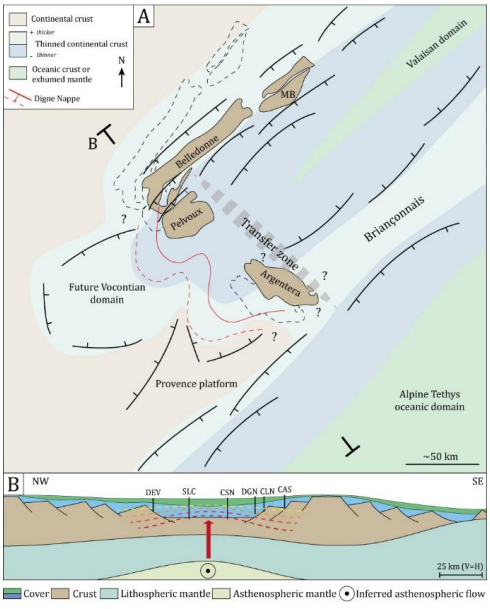

Figure 6: (A) Palaeogeographic reconstruction of the European margin in the Western Alps, during the Early Cretaceous after Graciansky and Lemoine (1988). Restored positions of the external crystalline massifs are after Bellahsen et al. (2014) and the Digne Nappe is restored based on shortening estimates from Ford et al. (2006). The SW Alps and the Digne Nappe were located in the continuation of the Valaisan rifted domain, as a result of the W-directed propagation of the Early Cretaceous rift system into the Vocontian Trough. MB = Mont Blanc massif. (B) Schematic reconstruction of the rifted margin through the study area, see location in (A). Dashed lines are notional isotherms.

We further notice that the choice of variable high-resolution thermal conductivities in the sedimentary cover results in relatively complex thermal gradients, such as higher geothermal gradients upsection with respect to samples at the base (Fig. 5). These results also indicate that high thermal gradients recorded in the upper part of the section may last for a longer period of time before temperature are relaxed to values consistent with gradients of 30°C/km (Fig. 5).

Tectonic reconstruction of Early Cretaceous rift in the SW Alps

The paleogeography of the SW Alps (Fig. 6) reveals that Jurassic – Early Cretaceous series of the Digne Nappe were originally located in the continuation of the Valaisan extensional domain, between the latter and the Vocontian Trough (Fig. 6A) (Lemoine et al., 1989; Beltrando et al., 2012; Dumont et al., 2012; Ribes et al., 2020; Dall'Asta et al., 2022). This continental rift zone appears to be separated from both the more mature continental margin of the Alpine Tethys and the Valaisan rift, by a transfer zone oriented NW-SE, parallel to extension, which is aligned along the eastern borders of Argentera and Pelvoux massifs (Lemoine et al., 1989). Numerical models of propagating rifts and spreading ridges show that such transitional domain can localize

https://doi.org/10.5194/egusphere-2022-949
Preprint. Discussion started: 20 September 2022

differential extension for tens of millions years before the rift actually propagates into the continent (Jourdon et al., 2020). Rift propagators are also sites of rift axis parallel asthenospheric flow (Mondy et al., 2018). In case of westward propagating rift in the SW Alps, asthenospheric mantle flow and lithosphere thinning are likely to be the main ingredient explaining the high thermal gradients during Late Jurassic – Early Cretaceous.

To the east of the Embrun half window, observed T_{max} are similar within the E-U nappes and the footwall series of the Digne Nappe (Fig. 2C). These temperatures are explained by a normal gradient of 30°C/km and nappe stacking of ca. 10 km when approaching the internal zones. The T_{max} gap observed at the NW front of the E-U nappes (Fig. 1B and 2C) reflects the overthrusting of the internally-derived E-U nappes and in contrast, also requires heating of the Jurassic series before emplacement of the E-U nappes. Based on our analysis of the Digne main thrust, those mid-crustal temperatures could reflect pre-Alpine heating, and temperatures inherited from the same Early Cretaceous thermal event. This implies that the thermal anomaly would not only be restricted to the Digne thrust front but must be of regional importance due to the structure of the European passive margin during the Mesozoic (Fig. 6).

CONCLUSION

Paleotemperatures of about 300°C reported at the front of the SW Alps are close to or even higher than paleotemperatures reported from the internal domains (e.g. Briançonnais). Basin modelling reveals that these mid-crustal temperatures are inherited from a long-lasting stretching process between Europe and Adria/Iberia with Tmax reached by lithospheric thinning event during the Early Cretaceous (130-110 Ma), and not related to crustal thickening during orogeny. As argued in the SW Alps, the recognition of collisional thermal events in accretionary prisms may therefore be elusive without a careful analysis of the pre-orogenic thermal evolution of the accreted units. The temperature structure reconstructed in orogens may therefore not illustrate nappe stacking or foreland deposition during collision, but instead represent pre-orogenic conditions. This can lead to overestimating both orogenic thickening and horizontal displacement in mountain belts. This issue is likely to be more significant in older orogenic systems where details of the original structural relationships are lacking. In the case of the Alps, the identification of Cretaceous thermal event places new constraints on the palaeogeographic reconstruction of the Alpine Tethys, kinematics and the rift architecture between the Europe and Adria.

https://doi.org/10.5194/egusphere-2022-949
Preprint. Discussion started: 20 September 2022

ACKOWLEDGEMENTS

This work has been supported by the Agence Nationale de la Recherche, Carnot Institute ISIFOR and the BRGM. We wish to thank Mary Ford for her comments in an earlier version of the manuscript. Beicip-Franlab is acknowledged for providing licences of the basin simulator TemisFlow™.

REFERENCES CITED

Angrand, P., and Mouthereau, F., 2021, Evolution of the Alpine orogenic belts in the Western Mediterranean region as resolved by the kinematics of the Europe-Africa diffuse plate boundary: BSGF - Earth Sciences Bulletin, v. 192, doi:10.1051/bsgf/2021031.

Barr, T.D., Dahlen, F.A., and McPhail, D.C., 1991, Brittle frictional mountain building: 3. Low-grade metamorphism: Journal of Geophysical Research, v. 96, doi:10.1029/91jb00295.

Baudrimont, F., and Dubois, P., 1977, Un bassin mésogéen du domaine péri-alpin : le sud-est de la France: Bulletin Centres Rech. Explor.-Prod. Elf-Aquitaine, v. 1, p. 261–308.

Bellahsen, N., Mouthereau, F., Boutoux, A., Bellanger, M., Lacombe, O., Jolivet, L., and Rolland, Y., 2014, Collision kinematics in the Western external Alps: Tectonics, v. 33, p. 1055–1088, doi:10.1002/2013TC003453.

Bellanger, M., Augier, R., Bellahsen, N., Jolivet, L., Monié, P., Baudin, T., and Beyssac, O., 2015, Shortening of the European dauphinois margin (Oisans Massif, Western Alps): New insights from RSCM maximum temperature estimates and 40Ar/39Ar in situ dating: Journal of Geodynamics, v. 83, p. 37–64, doi:10.1016/j.jog.2014.09.004.

Beltrando, M., Frasca, G., Compagnoni, R., and Vitale-Brovarone, A., 2012, The Valaisan controversy revisited: Multi-stage folding of a Mesozoic hyper-extended margin in the Petit St. Bernard pass area (Western Alps): Tectonophysics, v. 579, p. 17–36, doi:10.1016/j.tecto.2012.02.010.

Beltrando, M., Manatschal, G., Mohn, G., Vittorio, G., Piaz, D., Vitale, A., and Masini, E., 2014, Recognizing remnants of magma-poor rifted margins in high-pressure orogenic belts : The Alpine case study: Earth Science Reviews, v. 131, p. 88–115, doi:10.1016/j.earscirev.2014.01.001.

Célini, N., Callot, J., Pichat, A., Legeay, E., Graham, R., and Ringenbach, J., 2022, Secondary minibasins in orogens: Examples from the Sivas Basin (Turkey) and the sub-Alpine fold-and-thrust belt (France): Journal of Structural Geology, v. 156, p. 15, doi:10.1016/j.jsg.2022.104555.

Célini, N., Callot, J.-P., Ringenbach, J.-C., and Graham, R., 2021, Anatomy and evolution of the Astoin diapiric complex, sub-Alpine fold-and-thrust belt (France): BSGF - Earth Sciences Bulletin, v. 200052, p. 26, doi:https://doi.org/10.1051/bsgf/2021018.

Célini, N., Callot, J.-P., Ringenbach, J.-C., and Graham, R., 2020, Jurassic salt tectonics in the SW sub-Apine fold-and-thrust belt: Tectonics, v. 39, p. e2020TC006107, doi:10.1029/2020TC006107.

Clerc, C., and Lagabrielle, Y., 2014, Thermal control on the modes of crustal thinning leading to mantle exhumation: Insights from the cretaceous pyrenean hot paleomargins: Tectonics, v. 33, p. 1340–1359, doi:10.1002/2013TC003471.

Conand, C., Mouthereau, F., Ganne, J., Lin, A.T.S., Lahfid, A., Daudet, M., Mesalles, L., Giletycz, S., and Bonzani, M., 2020, Strain Partitioning and Exhumation in Oblique Taiwan Collision: Role of Rift Architecture and Plate Kinematics: Tectonics, v. 38, p. 1–30, doi:10.1029/2019TC005798.

Coward, M.P., and Dietrich, D., 1989, Alpine tectonics - an overview: Geological Society, London, Special Publications, p. 1–29.

Dall'Asta, N., Hoareau, G., Manatschal, G., Centrella, S., Denèle, Y., Ribes, C., and Kalifi, A., 2022, Structural and petrological characteristics of a Jurassic detachment fault from the Mont-Blanc massif (Col du Bonhomme area, France): Journal of Structural Geology, v. 159, p. 104593, doi:10.1016/j.jsg.2022.104593.

Debrand-Passard, S., Courbouleix, S., and Lienhardt, M.-J., 1984, Synthèse géologique du Sud-Est de la France, Mém. BRGM FR.: 1984 p.

Deville, É., and Sassi, W., 2006, Contrasting thermal evolution of thrust systems: An analytical and modeling approach in the front of the western Alps: AAPG Bulletin, v. 90, p. 887–907, doi:10.1306/01090605046.

Doligez, B., Bessis, F., Burrus, J., Ungerer, P., and Chenet, P.-Y., 1986, Integrated Numerical Simulation of Sedimentation, Heat transfer, Hydrocarbon formation and Fluid migration in a Sedimentary basin: The Themis model, *in* Thermal modelling in Sedimentary Basins, Proc. 1st IFP Research Conf. on

https://doi.org/10.5194/egusphere-2022-949
Preprint. Discussion started: 20 September 2022

Exploration, p. 173–195.
Ducoux, M., Jolivet, L., Masini, E., Augier, R., Lahfid, A., Bernet, M., and Calassou, S., 2021, Distribution and intensity of High-Temperature Low-Pressure metamorphism across the Pyrenean-Cantabrian belt: constraints on the thermal record of the pre-orogenic hyperextension rifting: BSGF - Earth Sciences Bulletin, v. 192, p. 43, doi:10.1051/bsgf/2021029.
Dumont, T., Schwartz, S., Guillot, S., Simon-Labric, T., Tricart, P., and Jourdan, S., 2012, Structural and sedimentary records of the Oligocene revolution in the Western Alpine arc: Journal of Geodynamics, v. 56–57, p. 18–38, doi:10.1016/j.jog.2011.11.006.
Dumont, T., Simon-Labric, T., Authemayou, C., and Heymes, T., 2011, Lateral termination of the north-directed Alpine orogeny and onset of westward escape in the Western Alpine arc: Structural and sedimentary evidence from the external zone: Tectonics, v. 30, p. 1–31, doi:10.1029/2010TC002836.
Faucher, T., Gidon, M., Pairis, J.-L., and Mascle, G., 1988, Directions de transport au front de la nappe de Digne (Chaînes subalpines méridionales): Comptes Rendus de l'Académie des Sciences de Paris, v. 306, p. 227–230.
Ford, M., Duchene, S., Gasquet, D., and Vanderhaeghe, O., 2006, Two-phase orogenic convergence in the external and internal SW Alps: Journal of the Geological Society, v. 163, p. 815–826, doi:10.1144/0016-76492005-034.
Fry, N., 1989, Southwestward thrusting and tectonics of the western Alps: Geological Society, London, Special Publications, v. 45, p. 83–109, doi:10.1144/GSL.SP.1989.045.01.05.
Gidon, M., 1997, Les chaînons subalpins au nord-est de Sisteron et l'histoire tectonique de la nappe de Digne: Géologie alpine, v. 73, p. 23–57.
Gidon, M., and Pairis, J.-L., 1985, La structure des environs de Digne (Chaînes subalpines méridionales, Alpes-de-Haute-Provence) : un exemple d'interférence entre l'avancée d'une nappe de charriage épiglyptique et la sédimentation sur son front: Comptes Rendus de l'Académie des Sciences de Paris, v. 307, p. 1283–1288, doi:0249-6305/88/03071283.
Graciansky, P.-C. de, Dardeau, G., Lemoine, M., and Tricart, P., 1989, The inverted margin of the French Alps and foreland basin inversion: Geological Society, London, Special Publications, v. 44, p. 87–104, doi:10.1144/GSL.SP.1989.044.01.06.
Graciansky, P.-C. de, and Lemoine, M., 1988, Early Cretaceous extensional tetonics in the southwestern French Alps: A consequences of North-Atlantic rifiting during Tethyan spreading: Bulletin de la Société Géologique de France, v. IV, p. 733–737.
Graham, R.H., Jackson, M.P.A., Pilcher, R., and Kilsdonk, B., 2012, Allochthonous salt in the sub-Alpine fold-thrust belt of Haute Provence, France, *in* Alsop, G.I., Archer, S.G., Hartley, A.J., Grant, N.T., and Hodkinson, R. eds., Salt Tectonics, Sediments and Prospectivity, Geological Society, London, Special Publications, 363, p. 595–615, doi:10.1144/SP363.30.
Haccard, D., Beaudoin, B., Gigot, P., and Jordan, M., 1989, Notice explicative, Carte géol. France (1/50 000), feuille La Javie (918), BRGM:
Handy, M.R., Schmid, S.M., Bousquet, R., Kissling, E., and Bernoulli, D., 2010, Reconciling plate-tectonic reconstructions of Alpine Tethys with the geological-geophysical record of spreading and subduction in the Alps: Earth-Science Reviews, v. 102, p. 121–158, doi:10.1016/j.earscirev.2010.06.002.
Izquierdo-Llavall, E., Menant, A., Aubourg, C., Callot, J.-P., Hoareau, G., Camps, P., Péré, E., and Lahfid, A., 2020, Pre-orogenic folds and syn-orogenic basement tilts in an inverted hyperextended margin: the northern Pyrenees case study:, doi:10.1029/2019tc005719.
Jensen, P.K., 1983, Calculations on the Thermal Conditions Around a Salt Diapir: Geophysical Prospecting, v. 31, p. 481–489, doi:10.1111/j.1365-2478.1983.tb01064.x.
Jourdan, S., Bernet, M., Tricart, P., Hardwick, E., Paquette, J.L., Dumont, T., and Schwartz, S., 2013, Short-lived, fast erosional exhumation of the internal western alps during the late early oligocene: Constraints from geothermochronology of pro-and retro-side foreland basin sediments: Lithosphere, v. 5, p. 211–225, doi:10.1130/L243.1.
Jourdon, A., Le Pourhiet, L., Mouthereau, F., and Masini, E., 2019, Role of rift maturity on the architecture and shortening distribution in mountain belts: Earth and Planetary Science Letters, v. 512, p. 89–99, doi:10.1016/j.epsl.2019.01.057.
Jourdon, A., Le Pourhiet, L., Mouthereau, F., and May, D., 2020, Modes of Propagation of Continental Breakup and Associated Oblique Rift Structures: Journal of Geophysical Research: Solid Earth, v. 125, p. 1–27, doi:10.1029/2020JB019906.
Kerckhove, C., and Thouvenot, F., 2010, Notice explicative, Carte géol. France (1/50 000), feuille Allos (919): Paris, Service de la Carte Géologique de France, 124 p.

https://doi.org/10.5194/egusphere-2022-949
Preprint. Discussion started: 20 September 2022

Labaume, P., Jolivet, M., Souquière, F., and Chauvet, A., 2008, Tectonic control on diagenesis in a foreland basin: Combined petrologic and thermochronologic approaches in the Grès d'Annot basin (Late Eocene-Early Oligocene, French-Italian external Alps): Terra Nova, v. 20, p. 95–101, doi:10.1111/j.1365-3121.2008.00793.x.

Lahfid, A., Beyssac, O., Deville, E., Negro, F., Chopin, C., and Goffé, B., 2010, Evolution of the Raman spectrum of carbonaceous material in low-grade metasediments of the Glarus Alps (Switzerland): Terra Nova, v. 22, p. 354–360, doi:10.1111/j.1365-3121.2010.00956.x.

Lanari, P., Guillot, S., Schwartz, S., Vidal, O., Tricart, P., Riel, N., and Beyssac, O., 2012, Diachronous evolution of the alpine continental subduction wedge: Evidence from P-T estimates in the Briançonnais Zone houillère (France - Western Alps): Journal of Geodynamics, v. 56–57, p. 39–54, doi:10.1016/j.jog.2011.09.006.

Lemoine, M. et al., 1986, The continental margin of the Mesozoic Tethys in the Western Alps: Marine and Petroleum Geology, v. 3, p. 179–199, doi:10.1016/0264-8172(86)90044-9.

Lemoine, M., Dardeau, G., Delpech, P.-Y., Dumont, T., de Graciansky, P.-C., Graham, R.H., Jolivet, L., Roberts, D., and Tricart, P., 1989, Extension syn-rift et failles transformantes jurassiques dans les Alpes Occidentales: Comptes Rendus de l'Académie des Sciences de Paris, v. 309, p. 1711–1716.

Lickorish, H.W., and Ford, M., 1998, Sequential restoration of the external Alpine Digne thrust system, SE France, constrained by kinematic data and synorogenic sediments: Geological Society, London, Special Publications, v. 134, p. 189–211.

Luisier, C., Baumgartner, L., Schmalholz, S.M., Siron, G., and Vennemann, T., 2019, Metamorphic pressure variation in a coherent Alpine nappe challenges lithostatic pressure paradigm: Nature Communications, v. 10, doi:10.1038/s41467-019-12727-z.

Manatschal, G., Chenin, P., Ghienne, J.F., Ribes, C., and Masini, E., 2021, The syn-rift tectono-stratigraphic record of rifted margins (Part I): Insights from the Alpine Tethys: Basin Research, v. 34, p. 457–488, doi:10.1111/bre.12627.

Manatschal, G., and Müntener, O., 2009, A type sequence across an ancient magma-poor ocean-continent transition: the example of the western Alpine Tethys ophiolites: Tectonophysics, v. 473, p. 4–19, doi:10.1016/j.tecto.2008.07.021.

Mello, U.T., Karner, G.D., and Anderson, R.N., 1995, Role of salt in restraining the maturation of subsalt source rocks: Marine and Petroleum Geology, v. 12, p. 697–716, doi:10.1016/0264-8172(95)93596-V.

Merle, O., and Brun, J.-P., 1984, The curved translation path of the Parpaillon Nappe (French Alps): Journal of Structural Geology, v. 6, p. 711–719, doi:10.1016/0191-8141(84)90010-5.

Mohn, G., Manatschal, G., Beltrando, M., and Haupert, I., 2014, The role of rift-inherited hyper-extension in Alpine-type orogens: Terra Nova, v. 26, p. 347–353, doi:10.1111/ter.12104.

Mondy, L.S., Rey, P.F., Duclaux, G., and Moresi, L., 2018, The role of asthenospheric flow during rift propagation and breakup: Geology, v. 46, p. 103–106, doi:10.1130/G39674.1.

Pleuger, J., and Podladchikov, Y., 2014, A purely structural restoration of the NFP20-East cross section and potential tectonic overpressure in the Adula nappe (central Alps): Tectonics, v. 33, p. 656–685, doi:10.1002/2013TC003409.

Rat, J., Mouthereau, F., Brichau, S., Crémades, A., Bernet, M., Balvay, M., Ganne, J., Lahfid, A., and Gautheron, C., 2019, Tectonothermal Evolution of the Cameros Basin: Implications for Tectonics of North Iberia: Tectonics, v. 38, p. 440–469, doi:10.1029/2018TC005294.

Ribes, C., Ghienne, J.F., Manatschal, G., Dall'Asta, N., Stockli, D.F., Galster, F., Gillard, M., and Karner, G.D., 2020, The Grès Singuliers of the Mont Blanc region (France and Switzerland): stratigraphic response to rifting and crustal necking in the Alpine Tethys: International Journal of Earth Sciences, v. 109, p. 2325–2352, doi:10.1007/s00531-020-01902-z.

Saspiturry, N., Lahfid, A., Baudin, T., Guillou-Frottier, L., Razin, P., Issautier, B., Le Bayon, B., Serrano, O., Lagabrielle, Y., and Corre, B., 2020, Paleogeothermal Gradients Across an Inverted Hyperextended Rift System: Example of the Mauléon Fossil Rift (Western Pyrenees): Tectonics, v. 39, doi:10.1029/2020TC006206.

Schwartz, S., Gautheron, C., Audin, L., Dumont, T., Nomade, J., Barbarand, J., Pinna-Jamme, R., and van der Beek, P., 2017, Foreland exhumation controlled by crustal thickening in the Western Alps: Geology, v. 45, p. 139–142, doi:10.1130/G38561.1.

Schwartz, S., Guillot, S., Reynard, B., Lafay, R., Debret, B., Nicollet, C., Lanari, P., and Auzende, A.L., 2013, Pressure-temperature estimates of the lizardite/antigorite transition in high pressure serpentinites: Lithos, v. 178, p. 197–210, doi:10.1016/j.lithos.2012.11.023.

Soret, M., Larson, K.P., Cottle, J., and Ali, A., 2021, How Himalayan collision stems from subduction:

https://doi.org/10.5194/egusphere-2022-949
Preprint. Discussion started: 20 September 2022

Geology, v. 49, p. 894–898, doi:10.1130/G48803.1.

Ternois, S., Mouthereau, F., and Jourdon, A., 2021, Decoding low-temperature thermochronology signals in mountain belts: Modelling the role of rift thermal imprint into continental collision: BSGF - Earth Sciences Bulletin, v. 192, p. 19, doi:10.1051/bsgf/2021028.

Tugend, J., Manatschal, G., Kusznir, N.J., and Masini, E., 2015, Characterizing and identifying structural domains at rifted continental margins: Application to the Bay of Biscay margins and its Western Pyrenean fossil remnants: Geological Society Special Publication, v. 413, p. 171–203, doi:10.1144/SP413.3.

Vacherat, A., Mouthereau, F., Pik, R., Bernet, M., Gautheron, C., Masini, E., Le Pourhiet, L., Tibari, B., and Lahfid, A., 2014, Thermal imprint of rift-related processes in orogens as recorded in the Pyrenees: Earth and Planetary Science Letters, v. 408, p. 296–306, doi:10.1016/j.epsl.2014.10.014.